ELSEVIER

International Journal of Solids and Structures 41 (2004) 4107–4120

INTERNATIONAL JOURNAL OF SOLIDS and STRUCTURES

www.elsevier.com/locate/ijsolstr

The electrical/thermal conductance of rough surfaces—the Weierstrass–Archard multiscale model

M. Ciavarella *, G. Murolo, G. Demelio

CEMEC-PoliBA, Centre of Excellence in Computational Mechanics, V.le Japigia 182, Politecnico di Bari, 70125 Bari, Italy

Received 3 September 2003; received in revised form 23 February 2004
Available online 28 March 2004

Abstract

Rough surfaces show a load-dependent electrical constriction resistance. Here, using a recent analogy due to Barber [Proc. R. Soc. London A 459 (2003) 53] between the incremental stiffness and the conductance in the elastic regime, and the Archard hypothesis to solve the multiscale contact problem, the conductance is found for the profile defined by the Weierstrass series. The analysis is also approximately valid, neglecting thermal effects on the contact area, for the thermal conductance.

Keywords: Electrical contact; Rough surfaces; Fractals

1. Introduction

The effect of roughness of real surfaces in contact mechanics is a problem of considerable importance in many areas of tribology. Greenwood and Williamson (1966) introduced asperity-based models, initially based on a set of identical asperities distributed according to Gaussian or exponential height distributions, providing one of the most convincing explanations of Amonton's law of friction in the elastic regime. Later studies used random process theory (Nayak, 1971; Whitehouse and Phillips, 1978; Greenwood, 1984) with the original intention to examine the relation between the various moments of the power spectrum (PS) which completely defines a Gaussian random process, and the properties of the peaks and summits. However, it has long been noticed that real profiles show multiscale features (Sayles and Thomas, 1978, Mandelbrot, 1982), and therefore the definition of asperity as local minima of the profile as suggested in "asperity-models" seems very questionable, as recognized by Greenwood himself recently in an "apology" paper (Greenwood and Wu, 2001). Because of their multiscale nature, fractal theories have been used for characterization of profiles and surfaces (Russ, 1994; Lopez et al., 1994), and more recent contact models are trying to consider more fully this effect. For example, Majumdar and Bhushan (1991, 1995) make a

* Corresponding author. Tel.: +39-080-596-2811; fax: +39-080-596-2777.
E-mail address: mciava@dimeg.poliba.it (M. Ciavarella).
URL: http://cemec.poliba.it/.

0020-7683/$ - see front matter © 2004 Elsevier Ltd. All rights reserved.
doi:10.1016/j.ijsolstr.2004.02.048

different definition of asperities based on the "bearing area" assumption (Johnson, 1985, p. 407) that the distribution of actual contact area sizes would be similar to that of the 'islands' generated by cutting through the surface at a constant height z, and use Mandelbrot's conjectures to estimate geometrically the distribution of diameters (the Korkac law). This leads to a finite contact area, but this contrasts with more detailed analysis of a fractal contact, showing a continuous decrease of the contact area when finer and finer scales are introduced, i.e. when the resolution of measurement is increased, and a limiting paradoxically *zero contact area* (Ciavarella et al., 2000; Borri-Brunetto et al., 1998). This in fact could be noticed already in the original Archard model (1957) as pointed out by Ciavarella and Demelio (2001). The paradoxical result opens up the question on whether the contact resistance is theoretically finite or not, and shows that a more rigorous analysis is needed of the contact mechanics, and the consequent electrical problem.

1.1. Electrical contact resistance

Electrical *contact* resistance is attributable to two sources: (i) the existence of thin films of poor conductors such as oxides at the interface and (ii) the *constriction resistance* associated with the roughness of the contacting surfaces. The effect of interfacial films can be minimized by the use of appropriate contacting materials, but surfaces are invariably rough on the microscopic scale and this results in the contact being restricted to a set of distributed, small, discrete actual contact areas. The electrical current has to pass through this geometric constriction, leading to an additional resistance attributable to surface roughness and known as constriction resistance.

Study of constriction resistance was pioneered by Holm (1958) and Greenwood (1966) who developed analytical expressions for the constriction resistance due to clusters of circular contact areas. The distribution of actual contact areas depends on the mechanics of the contact of rough surfaces and interest in electrical contact resistance was therefore an important motivating factor in the study of this subject. The contact of rough surfaces has itself proved to be a rich and challenging problem and the prediction of electrical resistance is still very much an inexact science.

If increased resolution in the surface roughness description leads to increasing numbers of progressively smaller contact areas, the constriction resistance associated with each individual contact area increases, but the sum of these resistances in parallel decreases, because this effect is dominated by the increased number of contacts. In the fractal limit, if we were to attribute the conductance to the parallel of isolated contact spots, we would be left with the paradoxical conclusion that the effective constriction resistance is unbounded (because the contact area goes to zero). This is the fractal equivalent of the observation above that with the constant of proportionality in the relationship between total contact area and applied load decreases with increasing resolution.

This conclusion is physically unrealistic on two counts: (i) at a sufficiently small scale, the intensity of loading on the individual asperities will cause plastic deformation, which will tend to establish finite sized contact areas as predicted by Majumdar and Bhushan (1991), and (ii) the constriction resistances associated with the individual contact areas cannot be regarded as being strictly in parallel since the latter will tend to be clustered in groups rather than uniformly distributed over the nominal contact area. Such clustering is a characteristic feature of fractal processes, see Mandelbrot (1982). Greenwood (1966) and Holm (1958) have shown how the resistance of clusters can be estimated and they conclude that for sufficiently dense clusters, the resistance tends to be equivalent to that of a single contact area enveloping the cluster rather than a parallel sum of the individual resistances.

In multiscale terms, this should lead us to expect that the total constriction resistance will approach a limit with increasing numbers of scales, even if elastic behavior is assumed throughout. However, the usefulness of the limit depends upon the rate at which it is approached with decreasing length scale. Suppose we define a length scale l_R below which the limit has been reached within reasonable engineering tolerances and a second length scale l_P below which plastic deformation or fracture is predicted in the

contact process (See Yan and Komvopoulos, 1998; Bhushan and Majumdar, 1992). The limiting value of resistance predicted by the elastic fractal model should then be a good approximation to the actual resistance as long as $l_P < l_R$. It should be noticed that in the case of significant plasticity, the classical model of Bowden and Tabor (1950) applies, since full yielding is predicted for *all* the asperities in contact, and the real contact area returns to be proportional to load, which was the first, classical explanation of Amonton's law for friction. In this paper we shall assume that the elastic assumption is valid, i.e. $l_P < l_R$.

More generally, we note that the fractal description of any physical phenomenon must become inapplicable at sufficiently small scale due to a variety of factors including changes in constitutive behavior, grain structure of the materials and atomic structure. The utility of the fractal description in any practical application depends upon whether the essential physics of interest is adequately characterized within the range of applicability. However, regardless of the answer to this question, it is generally desirable to use a surface characterization that does not contain an arbitrary (measurement precision determined) truncation limit.

1.2. Relation between the elastic and conduction problems

The elastic contact problem and the electrical conduction problem for the half space are closely related, because the corresponding Green's functions have the same mathematical form. Thus, the electrical potential due to a point current source on the surface and the normal displacement due to a point normal load on the surface both vary inversely with the distance from the source (load). It follows that the current distribution through any set of areas on the surface raised to a constant potential is proportional to the contact pressure required to cause the same set of areas to have a constant normal displacement. In a recent paper (Barber, 2003), this analogy was used to show a relationship between the electrical conduction problem and the elastic contact problem, demonstrating that the electrical conductance at any load is proportional to the incremental stiffness in the elastic contact problem. Indeed, Barber shows that the constriction resistance R is directly related to the derivative of the load F with respect to the displacement δ, by the following equation

$$\frac{1}{R} = \frac{2}{\rho^* E^*} \frac{\mathrm{d}F}{\mathrm{d}\delta}, \tag{1}$$

where

$$\frac{1}{E^*} = \frac{1-\nu_1^2}{E_1} + \frac{1-\nu_2^2}{E_2}, \quad \rho^* = \rho_1 + \rho_2 \tag{2}$$

are combined elastic modulus and combined resistivities of the materials, and ν is Poisson's ratio. A corollarium of Barber's analogy is that, for a finite roughness peak-to-valley amplitude s of the combined roughness, the constriction resistance is finite, regardless on the details of the surfaces.

It follows that if we can solve the frictionless contact problem, we do not need to perform an additional calculation to find the contact resistance—indeed, the contact resistance can be written down even for the non-linear case where there is also heat conduction and the electrical resistivity is temperature-dependent (see Jang et al., 1998). Of course, this does not by-pass the problem of the interaction terms, since the same terms appear in the formulation of the elastic contact problem. It should be noticed, however, that interaction terms are significantly more important when the resolution is increased. In other words, if a simple calculation is made based essentially on the bearing area assumption, a poor estimate is made over the effective contact area, but a generally satisfactory estimate is made of mechanical compliance (and therefore of electrical resistance, by virtue of the electro-mechanical analogy). More precisely, if we take the original Greenwood–Williamson model with *identical* and independent asperities, with the simplest of ϕ, the exponential distribution function of asperity heights (Johnson, 1985, Section 13.4), a simple result is obtained by using the analogy, that the conductance is predicted to be linear with total load

$$C_{\mathrm{GW}} = \frac{1}{R_{\mathrm{GW}}} = \frac{2}{\rho^* E^*} \frac{F}{\sigma_s}, \tag{3}$$

showing that the only asperity feature which seems to matter for the electrical conductance is the amplitude parameter of summit height σ_s (and not of summit slopes and curvatures) of the exponential distribution (this should not be confused with the RMS height of a Gaussian distribution). The latter is expected to vary only moderately with sample length L and is nearly independent on sampling interval. Vice versa, the relationship between load and separation would involve the local features of asperities, the curvature in particular, and would therefore strongly depend on resolution. With a more realistic Gaussian distribution, the relationships cease to be so simple and closed form, but the general trend remains similar.

Another class of models start from the Bowden and Tabor (1950) plastic model for mechanical contact, linking the area of contact A_{c} and Hardness H of the material as

$$F = A_{\mathrm{c}} H. \tag{4}$$

Defining the Holm radius as the radius of an equivalent spot such that the resistance is $R_{\mathrm{c}} = \rho/2\alpha$, and estimating it from the area of contact A_{c} and an empirical coefficient η of order unity for clean interfaces,

$$A_{\mathrm{c}} = \eta \pi \alpha^2 \tag{5}$$

then the resistance is

$$C_{\mathrm{BT}} = \frac{1}{R_{\mathrm{BT}}} = \sqrt{\frac{4F}{\rho^2 \eta \pi H}}. \tag{6}$$

Notice how the plastic exponent of the relation conductance-load is much smaller than the elastic coefficient for rough surfaces (1/2 instead of 1). A single Hertzian contact obviously would imply an even smaller exponent, $C_H \sim F^{1/3}$. The exponent therefore can vary largely, and is strongly dependent on the geometrical and mechanical features of the contact.

Traditional treatments of contact resistance include a wide variety of empirical and semi-empirical treatments, combining in turn two or more of these three basic components, roughness, plasticity, single contact laws (including for example attempts to include the effect of hardness variation with size), plus a series of corrective factors to take into account at times of films, oxides, etc. Most of them use statistical surface parameters largely dependent on resolution (Tien, 1968; Cooper et al., 1969; Mikic, 1974; Yovanovich, 1987), and therefore should be used with great care when the original assumptions are not satisfied (particularly in the use of microscopic constitutive laws which depend strongly on the determination of asperity contacts size). For a quite extensive review (although dedicated to thermal contact conductance instead of electrical conductance), see Lambert and Fletcher (1997), and the references therein. One original model using fractal geometry for the surface characterization, was introduced also for electrical contact (Majumdar and Tien, 1991), but using a network of resistances in series and parallel, where the assumed patterns are based on properties of the surface profiles independently of the contact process.

1.3. Outline of the paper

This paper is concerned with the contact defined by the deterministic fractal Weierstrass profile (Weierstrass, 1895, Berry and Lewis, 1980) with fractal dimension $D \in [1, 2]$, defined by the series of sine waves

$$z(x) = \sum_{n=0}^{\infty} g_n \cos\left(\frac{2\pi x}{\lambda_n}\right); \quad g_n = g_0 \gamma^{(D-2)n}; \quad \frac{\lambda_0}{\lambda_n} = \gamma^n, \tag{7}$$

where g_0, λ_0 are constants with dimensions of length and $\gamma > 1$, $D > 1$ are dimensionless constants. The first, γ, is the parameter giving the wavelength ratio in the geometric progression, and D is the fractal

dimension. Ciavarella et al. (2000) then showed that the contact area has *limiting* fractal dimension between 1 and 2, and which only depends on the geometry D.

Archard's technique is a perfect match for the Weierstrass series with large γ values. Clearly, the Weierstrass series has a discrete power spectral density instead of the continuous law which is more generally expected for real surfaces, whereas the structure function is continuous. Various extensions of the original Weierstrass series are known (Mandelbrot, 1982; Lopez et al., 1994) to make the function more realistic. Despite these possible criticisms, however, it should be noticed that:

(1) having a discrete spectrum makes it easier to define, in engineering terms, the boundaries between "form", "waviness" and "roughness", by simply picking up the appropriate terms of the series, instead of having to integrate over ranges of wavelength in a given power spectrum;
(2) a continuous power law of the form $P(\omega) = C\omega^{-q}$ needs in practise some truncation at low wavenumbers, where it must show a limit constant cutoff. This is automatically included in the Weierstrass series, without any confusion because of the implied truncation of the first sinusoidal wave;
(3) even if the continuous power spectrum may be the best representation, and even if the profile is really Gaussian, it is not clear if the contact process should depend only on the moments of the PS;
(4) the use of $\gamma \gg 1$ permits to avoid the introduction of random phase variables, and ensemble averaging processes.

Fig. 1 shows some example plots of Weierstrass series. It is clear that the larger γ, the more deterministic becomes the surface, with clearly distinguishable contributions of the various sinusoidal terms.

In this paper, we shall extend the results of Ciavarella et al. (2000) to the load-displacement relationship, which, in light of the recent paper by Barber (2003), can also immediately provide an estimate of the electrical and thermal conductance in the elastic regime.

2. The Weierstrass–Archard model

Consider a two-dimensional elastic half-plane indented by a rigid body with the Weierstrass series profile (7) which is bounded in the range $-G_t < z(x) < G_t$, where

$$G_t = \frac{g_0}{1-\gamma^{(D-2)}}. \tag{8}$$

For a load $P = p_{-1}\lambda_0 = p_{-1}L$, the single wave solution (Johnson, 1985, 13.2) gives full contact for a mean pressure $p_{-1} \geqslant p_0^* = \frac{\pi E}{1-\nu^2}\frac{g_0}{\lambda_0}$. Superposition for the Weierstrass series suggests that

$$p(x) = p_{-1} + p^* \cos\left(\frac{2\pi x}{\lambda}\right), \tag{9}$$

where

$$p^* = \sum_{n=0}^{N} p_n^* = p_0^* \sum_{n=0}^{N} \gamma^{(D-1)n}. \tag{10}$$

Since the series doesn't converge, as $p^* \to \infty$ for $N \to \infty$, full contact is reached only in the limit of infinite pressure, and there will be regions of separation for *all finite applied loads*.

The Archard hypothesis to solve the partial contact problem is to suppose that $\gamma \gg 1$, so that there are many waves of scale n in one wavelength of scale $n-1$, and the effect of the various scales can be decoupled. This permitted Ciavarella et al. (2000) to use the Westergaard solution to find that at scale n the peak pressure is given by the iteration

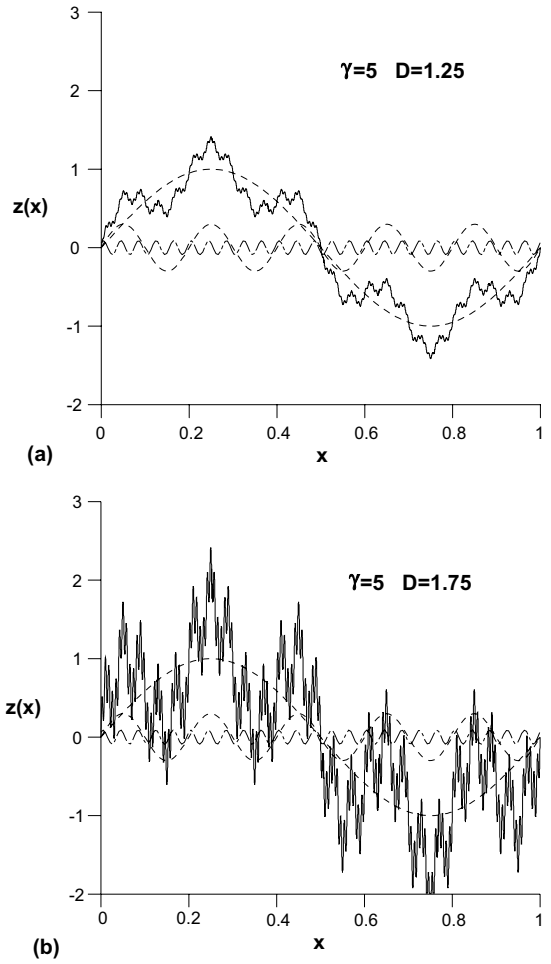

Fig. 1. (a) The continuous plot is the Weierstrass series for $g_0 = 1$, $\lambda_0 = 1$, $\gamma = 5$ and $D = 1.25$. The dashed lines are the first three wave of the series. (b) The continuous plot is the Weierstrass series for $g_0 = 1$, $\lambda_0 = 1$, $\gamma = 5$ and $D = 1.75$. The dashed lines are the first three wave of the series.

$$\frac{p_n^{\max}}{p_n^*} = f(x_{n-1}), \quad x_{n-1} = \frac{p_{n-1}^{\max}}{p_n^*}, \tag{11}$$

where

$$f(x) = 1 + x, \quad x > 1, \tag{12}$$

$$f(x) = 2\sqrt{x}, \quad 0 > x > 1. \tag{13}$$

The iteration converges, *for sufficiently large n*, for $\gamma^{D-1} > 2$ to partial contact, and for $\gamma^{D-1} < 2$ to full contact, but these regions become a vanishingly small proportion of the total number of asperity contacts as n increases and their sizes decrease at each scale. Obtaining the iterative process shown graphically in Fig. 2.

Fig. 2 shows a graphical iteration of the form ABCD defined by

$$x_n = \gamma^{1-D} f(x_{n-1}), \tag{14}$$

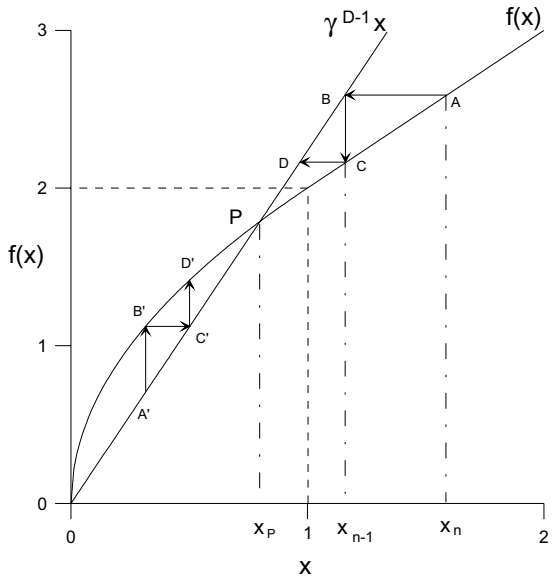

Fig. 2. The graphical iteration defined by Eq. (11).

which converges monotonically on the unique positive non-zero solution of the equation

$$x = \gamma^{1-D} f(x), \tag{15}$$

for any positive starting value x_0. The solution of Eq. (15) corresponds to the point P in Fig. 2, where the straight line has slope γ^{D-1}. Solving for x_{P}, we obtain

$$x_{\mathrm{P}} = \frac{4}{\gamma^{2(D-1)}} < 1, \quad \gamma^{D-1} > 2 \text{ “partial contact”}, \tag{16}$$

$$x_{\mathrm{P}} = \frac{1}{\gamma^{D-1} - 1} > 1, \quad \gamma^{D-1} < 2 \text{ “full contact”}, \tag{17}$$

where “full contact” and “partial contact”, respectively, is intended as the condition at the peaks on peaks..., only. Fig. 3(a) shows the point x_P as a function of varying γ and for several fractal dimension. It is immediate to realize that the boundary $x_P = 1$ corresponds to $\gamma^{D-1} = 2$. Notice that $\gamma^{D-1} > 2$ means $\gamma > 16$ for $D = 1.25$, but $\gamma > 4$ for $D = 1.5$, and finally $\gamma > 2^{4/3} = 2.52$ for $D = 1.75$.

Hence, because the iteration is monotonic, when we start with $x_0 < x_P$, the x values will increase whereas for with $x_0 > x_P$, the x values will decrease. It follows that:

- for $x_P > 1$ (i.e. $\gamma^{D-1} < 2$), if we start with $x_0 = 1$ or larger (full contact), we remain above unity, suggesting *full contact at the peaks at all scales*. If we start from light loads $x_0 < 1$, we will get increasingly close to full contact (at the peaks), and eventually we would converge to full contact. From the results in Fig. 3(a), it is clear that this will be the case for small γ and D, whereas only for large γ and D, we will get the second possibility, i.e.
- for $x_P < 1$ (i.e. $\gamma^{D-1} > 2$); if we start with $x_0 = 1$ or larger, we may remain for few scales at full contact, but we end up with partial contact even at the peaks *at a sufficiently large n*. If we start from $x_P < x_0 < 1$,

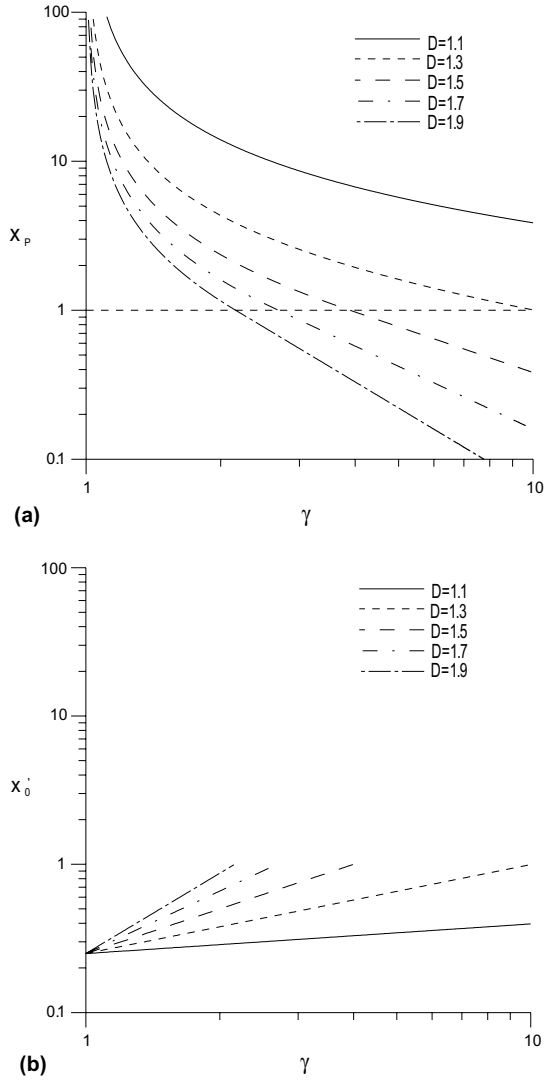

Fig. 3. The points x_p (a) and the point x_0' (b) as a function of γ in the range from 1 to 10, and for various $D = 1.1, 1.3, 1.5, 1.7, 1.9$.

we will decrease the ratio x and then converge to x_P, and finally for sufficiently light loads $x_0 < x_P < 1$, we will remain at $x_P < 1$ at all scales. In particular, Hertzian regime could be considered for $x < 0.2$.

The full contact parameter range deserves some comment, since regions of full contact will be increasingly smaller at smaller scales. This may lead to inaccuracies when computing the compliance, since we will make our calculations based on asperity peaks condition. To see how many iterations are needed to converge in this range to full contact, one can start by looking when 2 scales are enough to converge. To find the maximum pressure needed to converge, we use Eq. (14), with $x_1 = 1$, obtaining

$$x_0' = \frac{1}{4}\gamma^{2(D-1)}, \tag{18}$$

and Fig. 3(b) plots this result as a function of γ and for various dimensions D, following the same examples as Fig. 3(a) (notice that the lines are truncated at $\gamma^{D-1}=2$ which is the limit range and which gives in fact $x_0'=1$). Similarly, to find the limit pressure to get convergence to full contact at the third scale, one uses this value as minimum value at the second scale, $x_1=\frac{1}{4}\gamma^{2(D-1)}$, obtaining in turn

$$\frac{1}{4}\gamma^{2(D-1)}=\gamma^{1-D}2\sqrt{x_0''}, \tag{19}$$

which gives

$$x_0''=\frac{1}{64}\gamma^{6(D-1)} \tag{20}$$

and so on.

Turning back on the main issue of the paper, the calculation of the compliance, we shall reason in the spirit of the original Archard hypothesis of no-redistribution of load. Infact, the compliance is obtained by summing the compliance at each scale, considering always the most deformed locations, i.e. the peaks on peaks..., having from the results in Appendix A,

$$\left(\frac{\delta}{g}\right)_n=\frac{p_{n-1}^{\max}}{p_n^*}\left\{1-\ln\left(\frac{p_{n-1}^{\max}}{p_n^*}\right)\right\}=x_{n-1}\{1-\ln x_{n-1}\},\quad x_{n-1}<1, \tag{21}$$

$$\left(\frac{\delta}{g}\right)_n=\frac{p_{n-1}^{\max}}{p_n^*}\left\{1-\ln\left(\frac{p_{n-1}^{\max}}{p_n^*}\right)\right\}=1,\quad x_{n-1}\geqslant 1 \tag{22}$$

and

$$\delta=\sum_{n=0}^{\infty}\delta_n=\sum_{n=0}^{\infty}g_n\left(\frac{\delta}{g}\right)_n. \tag{23}$$

For the most likely parameter range $\gamma^{D-1}<2$, we simply obtain that

$$\left(\frac{\delta}{g}\right)_n=1,\quad \text{for all } n,\quad \text{for } x_0=\bar{p}/p_0^*\geqslant 1 \tag{24}$$

i.e.

$$\delta=\sum_{n=0}^{\infty}g_n=G_t,\quad \text{for } x_0=\bar{p}/p_0^*\geqslant 1. \tag{25}$$

We now turn to make use of Barber's analogy (Barber, 2003), and specializing (1) to a 2D problem in terms of pressure instead of force $F=\bar{p}A_0$, with $A_0=\lambda_0 t$ where λ_0 is the longest wavelength and t is the thickness, reads

$$\frac{1}{R}=\frac{2}{\rho^*E^*}\frac{\mathrm{d}F}{\mathrm{d}d}=\frac{2\lambda_0 t}{\rho^*E^*}\frac{\mathrm{d}\bar{p}}{\mathrm{d}\delta}. \tag{26}$$

In particular,

$$R\equiv\frac{\mathrm{d}\delta}{\mathrm{d}\bar{p}}=0,\quad \text{for}\quad x_0=\bar{p}./p_0^*\geqslant 1 \tag{27}$$

Remaining in the parameter range $\gamma^{D-1}<2$, but for lower pressures $x_0<1$, the first few scales will give a partial contribution, with an increasingly larger percentage $\left(\frac{\delta}{g}\right)_n$, but eventually the series will converge to

$$\left(\frac{\delta}{g}\right)_n = 1, \quad \text{for all } n \text{ for which } x_n \geqslant 1. \tag{28}$$

Moving to the parameter range $\gamma^{D-1} > 2$, for any applied pressure, there will be some scale where the $\left(\frac{\delta}{g}\right)_n < 1$, but these will be an increasingly smaller factor for large enough pressures. Clearly, the larger γ^{D-1} the slower the convergence towards the limit G_t will be with pressure, and accordingly, the slower the decay of resistance to the zero limit.

3. Results

In making the comparisons, we fix the first term amplitude, g_0, and show the results of total displacements at peaks on peaks in dimensionless terms by dividing for the maximum amplitude (8) which will give the upper value obtained asymptotically for full contact. Notice that the Archard assumption will lead to "full contact" at the peaks, as from the previous paragraph, for the range $x_P > 1$ (i.e. $\gamma^{D-1} < 2$), whereas it is clear that the Weierstrass series will never lead to a true full contact, if not asymptotically for infinite pressure. Obviously, it cannot be exact because even in this range, full contact is lost progressively. However, the contact area is not the best way to judge the resistance as it takes no account of clustering. Vice versa, our assumption simply gives high relevance to clustering effect, and is believed to be a good approximation (or probably the best without involving a full numerical solution to the problem).

Also, notice that not necessarily the range $\gamma^{D-1} > 2$ leads to more accurate results. In Fig. 4 then we present both displacement and resistance results for the case $\gamma = 3$, 5, 10, and $D = 1.25$, 1.75, i.e. for the lower D full contact, and in the higher D partial contact. The curves are plotted as a function of $\frac{\bar{p}}{p_0^*}$ where p_0^* is the pressure to flatten the first sinusoidal wave, and $\bar{p}$ is the nominal average pressure. Notice that since the curves are obtained for the same first term amplitude, $g_0 = 1$, but are plotted in terms of δ/G_t where $G_t = g_0 = 1$ in the case of the single sinusoid and otherwise it depends on both γ, D as given in (8). The various curves clearly show for very large γ, the curves tend to the single sinusoid case.

Also, notice that we present the resistance in terms of non-dimensional values R/R_0 where

$$R_0 = \frac{\rho^*}{2t}. \tag{29}$$

Included in the figures is also the case of a single sinusoid ($\gamma = \infty$), for which the resistance is obtained in closed form as

$$\frac{\mathrm{d}\delta}{\mathrm{d}p} = g\frac{\mathrm{d}}{\mathrm{d}p}\left[\frac{p}{p^*}\left\{1 - \ln\left(\frac{p}{p^*}\right)\right\}\right] = -\frac{g}{p^*}\ln\left(\frac{p}{p^*}\right) \tag{30}$$

and so

$$\frac{R}{R_0} = -\frac{1}{\pi}\ln\left(\frac{p}{p^*}\right), \tag{31}$$

for comparative purposes. It can be noticed that for low fractal dimensions the curves are close to each other, indicating a minor effect of γ. For low pressures, the resistance tends to be higher than the single sinusoid case, whereas at larger pressures, the trend is opposite and finally they all tend to converge to apparent full contact (zero resistance) at $\frac{\bar{p}}{p_0^*} = 1$. Notice that the larger γ, the closer the various profiles are to the single sinusoid case. This may appear surprising, but it is in fact legitimate as given the various amplitudes become negligible for large γ and large D, it is expected that the Archard hypothesis becomes asymptotically correct to the obvious result!

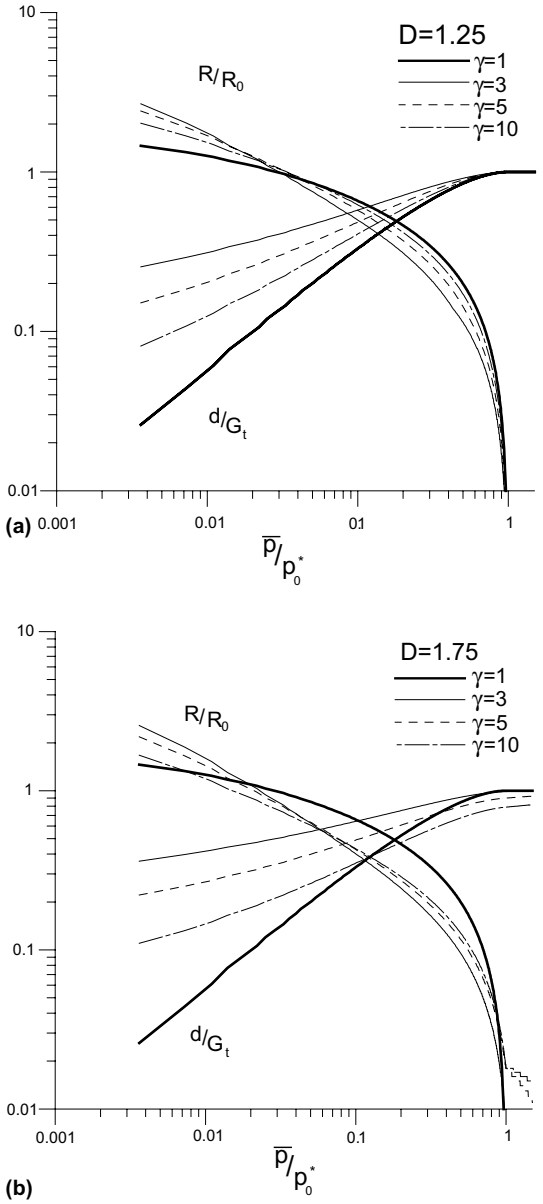

Fig. 4. (a) Results for the dimensionless value of resistance and total displacement for the Weierstrass series for $g_0 = 1$, $\lambda_0 = 1$, $D = 1.25$ and various $\gamma = 1, 3, 5, 10$. (b) Results for the dimensionless value of resistance and total displacement for the Weierstrass series for $g_0 = 1$, $\lambda_0 = 1$, $D = 1.75$ and various $\gamma = 1, 3, 5, 10$.

It is clear that all other curves tends to the linear behavior (in the logarithmic scale, i.e. power law) at small pressures, and eventually lead to zero resistance around $\frac{p}{p^*} = 1$ (whereas the single sinusoid doesn't). From the results, it is evident that the resistance curves show a smaller variation than the compliance laws. This is probably due to the effect of derivation, and also to the fact that, despite the "partial contact" high fractal dimension cases ($D = 1.75$) never converge to the full contact sum $\left(\frac{\delta}{g}\right)_n = 1$, they are also the cases

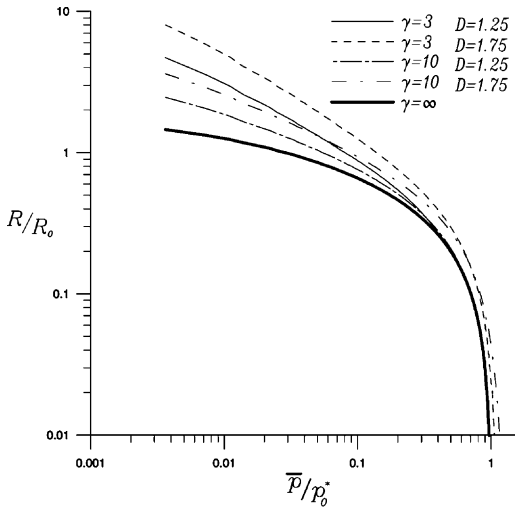

Fig. 5. Results for the dimensionless resistance for the Weierstrass series for various parameters.

for which the g_n terms most rapidly decay to zero. Therefore, while at low pressures the multiscale cases show higher resistance than the single sinusoid, at larger pressures, the resistance becomes lower, and eventually they nearly converge at the same loads to full contact/zero resistance.

Additionally, in Fig. 5 we show a synthesis of the results for resistance only. Notice that at small loads there is a power law dependence with load, but it seems that the exponent is not necessarily equal in all conditions.

4. Conclusions

The Archard model as applied to the Weierstrass series permits to devise a simple approximate method to compute the electrical resistance of a multiscale, fractal deterministic profile, by using the Barber analogy with interface stiffness and assuming the stiffness depends only on the displacements of the peaks on peaks on peaks. The results have been shown for a range of parameters γ, D of the Weierstrass series. Within the Archard assumption, the result show that the effect of varying the parameters in terms of resistance is not as large as expected, since the main contribution comes from the biggest sinusoidal term. This confirms that the macroscopic features dominate the problem, as it was already suggested by Barber (2003), and deviations occur at small loads where roughness increases the resistance, and cause the dependence to be of power law type with load.

Acknowledgements

The authors are pleased to acknowledge support from the EC under the project AUTOCON.

Appendix A. The Westergaard solution

The Westergaard solution (Westergaard, 1939) is obtained in the form

$$2\mu u_x = (1-v)\Re(\psi) - y\Im(\phi), \tag{A.1}$$

$$2\mu u_y = 2(1-v)\Im(\psi) - y\Re(\phi), \tag{A.2}$$

where μ, v are the modulus of rigidity and Poisson's ratio respectively, and

$$\phi = \frac{\partial \psi}{\partial z}, \tag{A.3}$$

where

$$z = x + \mathrm{i}y \tag{A.4}$$

is the complex variable. The stress function

$$\phi = -\frac{2p\cos\zeta}{\sin^2\zeta}\left\{\sqrt{\sin^2\alpha - \sin^2\zeta} + \mathrm{i}\sin\zeta\right\}, \tag{A.5}$$

where

$$\zeta = \frac{\pi z}{\lambda}, \tag{A.6}$$

also, p is the mean contact pressure

$$\alpha = \frac{\pi\alpha}{\lambda} \tag{A.7}$$

and a is the semi-width of the contact area.

To evaluate the compliance of the system, we first substitute (A.5) into (A.3) and integrate, obtaining

$$\psi = -\frac{p\lambda}{\pi}\left\{\frac{\sin\zeta\sqrt{\sin^2\alpha - \sin^2\zeta}}{\sin^2\alpha} + \arctan\left[\frac{\sin\zeta}{\sqrt{\sin^2\alpha - \sin^2\zeta}}\right] + \frac{\mathrm{i}\sin^2\zeta}{\sin^2\alpha}\right\}. \tag{A.8}$$

After some complex algebra, we can then find that at large y,

$$2\mu u_y(0,y) \to -(1-2v)py - \frac{(1-v)p\lambda}{\pi}\{1 - 2\ln(\sin\alpha)\}, \tag{A.9}$$

whilst

$$2\mu u_y(0,0) = 0. \tag{A.10}$$

The first term in (A.9) is the displacement associated with a uniform hydrostatic stress p and we need to subtract this to find the additional compliance due to roughness, which is

$$\delta = \frac{(1-v)p\lambda}{2\mu\pi}\{1 - 2\ln(\sin\alpha)\}. \tag{A.11}$$

We can also express $\sin\alpha$ in terms of the pressure p as

$$\sin\alpha = \sqrt{\frac{p}{p^*}}, \tag{A.12}$$

where p^* is the mean pressure required to completely flatten the roughness and is given by

$$p^* = \frac{2\pi\mu g}{\lambda(1-v)}, \tag{A.13}$$

where g is the amplitude of the sinusoidal roughness. Using this result, we have

$$\frac{\delta}{g} = \frac{p}{p^*}\left\{1 - \ln\left(\frac{p}{p^*}\right)\right\}. \tag{A.14}$$

Notice that the maximum compliance due to the roughness is g and this occurs when $p = p^*$. For all larger values of p, the compliance remains unchanged, since there is then full contact and only the hydrostatic component of stress changes.

References

Archard, J.F., 1957. Elastic deformation and the laws of friction. Proc. R. Soc. London A 243, 190–205.

Barber, J.R., 2003. Bounds on the electrical resistance between contacting elastic rough bodies. Proc. R. Soc. (London) A 459, 53–66.

Berry, M.V., Lewis, Z.V., 1980. On the Weierstrass–Mandelbrot fractal function. Proc. R. Soc. Lond. A 370, 459–484.

Borri-Brunetto, M., Carpinteri, A., Chiaia, B., 1998. Lacunarity of the contact domain between elastic bodies with rough boundaries. In: Frantziskonis, G. (Ed.), Probamat-21st Century: Probabilities and Materials. Kluwer, Dordrecht, pp. 45–64.

Bowden, F.P., Tabor, D., 1950. Friction and Lubrication of Solids. Clarendon Press, Oxford, UK.

Bhushan, B., Majumdar, A., 1992. Elastic plastic model for bifractal surfaces. Wear 153 (1), 53–64.

Ciavarella, M., Demelio, G., Barber, J.R., Jang, Y.H., 2000. Linear elastic contact of the Weierstrass profile. Proc. R. Soc. (London) A 456, 387–405.

Ciavarella, M., Demelio, G., 2001. Elastic multiscale contact of rough surfaces: Archard's model revisited and comparisons with modern fractal models. J. Appl. Mech. Trans. ASME 68, 496–498.

Cooper, M.G., Mikic, B.B., Yovanovich, M.M., 1969. Thermal contact conductance. Int. J. Heat Mass Transfer 12, 279–300.

Greenwood, J.A., 1966. Constriction resistance and the area of real contact. Br. J. Appl. Phys. 17, 1621–1632.

Greenwood, J.A., 1984. A unified theory of surface roughness. Proc. R. Soc. London A 393, 133–157.

Greenwood, J.A., Williamson, J.B.P., 1966. The contact of nominally flat surfaces. Proc. R. Soc. London A 295, 300–319.

Greenwood, J.A., Wu, J.J., 2001. Surface roughness and contact: an apology. Meccanica 36 (6), 617–630.

Holm, R., 1958. Electrical Contacts Handbook. Springer–Verlag, Berlin.

Jang, Y.H., Barber, J.R., Hu, S.J., 1998. Electrical conductance between dissimilar materials with temperature-dependent properties. J. Phys. D: Appl. Phys. 31, 3197–3205.

Johnson, K.L., 1985. Contact Mechanics. Cambridge University Press, Cambridge.

Lambert, M.A., Fletcher, L.S., 1997. Review of models for thermal contact conductance of metals. J. Thermophys. Heat Transfer 11 (2), 129–140.

Lopez, J., Hansali, G., Le Bossé, J.C., Mathia, T., 1994. Caracterisation fractale de la rugosité tridimensionelle d'une surface. J. Phys. III (France) 4, 2219–2501.

Majumdar, A., Bhushan, B., 1991. Fractal model of elastic–plastic contact between rough surfaces. ASME J. Tribology 113, 1–11.

Majumdar, A., Bhushan, B., 1995. Characterization and modeling of surface roughness and contact mechanics. In: Handbook of Micro/Nano Tribology. CRC Press, New York, pp. 109–165.

Majumdar, A., Tien, C.L., 1991. Fractal network model for contact conductance. ASME J. Heat Transfer 113, 516–525.

Mandelbrot, B.B., 1982. The Fractal Geometry of Nature. Freeman, San Francisco.

Mikic, B.B., 1974. Thermal contact conductance; theoretical considerations. Int. J. Heat Mass Transfer 17 (Feb), 205–214.

Nayak, P.R., 1971. Random process model of rough surfaces. ASME J. Lubrication Technol. 93, 398–407.

Russ, J.C., 1994. Fractal Surfaces. Plenum Press, New York.

Sayles, R.S., Thomas, T.R., 1978. Surface topography as a nonstationary random process. Nature 271, 431–434.

Tien, C.L., 1968. A Correlation for Thermal Contact Conductance of Nominally Flat Surfaces in Vacuum. In: Proceedings of the 7th Thermal conductivity Conference. US Bureau of Standards, pp. 755–759.

Weierstrass, K., 1895. Mathematische Werke. Mayer and Muller, Berlin.

Westergaard, H.M., 1939. Bearing pressures and cracks. ASME J. Appl. Mech. 6, 49–53.

Whitehouse, D.J., Phillips, M.J., 1978. Discrete properties of random surfaces. Philos. Trans. R. Soc. London, A 290, 267–298.

Yan, W., Komvopoulos, K., 1998. Contact analysis of elastic–plastic fractal surfaces. J. Appl. Phys. 84 (7), 3617–3624.

Yovanovich, M.M., 1987. Theory and applications of constriction and spreading concepts for microelectronic thermal management. Keynote Address, In: Proceedings of the International Symposium on Cooling Technology for Electronic Equipment, Honolulu, HI.